

Investigating the Performance of Different Window Opening Styles for Single-Sided Wind-Driven Natural Ventilation Using CFD Simulations

Akshit Gupta – Eurac Research, Italy – akshit.gupta@eurac.edu

Annamaria Belleri – Eurac Research, Italy – annamaria.belleri@eurac.edu

Francesco Babich – Eurac Research, Italy – francesco.babich@eurac.edu

Abstract

Natural ventilation can be an effective means of providing healthy and comfortable indoor environments while minimizing energy consumption. However, the use of diverse types of windows and control strategies usually leads to different indoor local thermal conditions. Previous studies have focused on indicators of ventilation effectiveness, but too little is known about the spatial variations of thermal comfort generated by different window opening styles. CFD is a powerful numerical modeling technique to compare the air distribution within a room, and therefore to evaluate the performances of different type of window in terms of delivered thermal comfort and indoor air quality (including local effects). Thus, the aim of this research is to investigate the effectiveness of diverse type of window, such as bottom-hung, horizontal pivot and top-hung fanlight for single-sided wind-driven natural ventilation. In this study, two wind speeds and two wind-window angles were investigated, for two weather conditions typical for the region of South Tyrol, Italy. In this study, thermal comfort was evaluated based on standards EN ISO 7730 and ASHRAE Standard 55. Using transient RANS CFD simulations, the performance of different window configurations for the different boundary conditions were numerically evaluated. The boundary conditions, geometrical simplifications, grid-independence tests, discretization, and basic principles for a transient simulation were chosen based on previous studies and then tested to ensure the correct modelling of a wind-driven natural ventilation flow. The results show 25 %-200 % higher incoming airflow when the wind enters at an acute angle as compared with perpendicular wind. Furthermore, the horizontal-pivot window reports a 39 % higher incoming airflow when compared with bottom-hung window style, while the draught risk in winter conditions was similar for both.

1. Introduction

Across the world, buildings are a big consumer of energy. In the EU alone, buildings account for 40 % of our energy consumption and 36 % of greenhouse gas emissions (European Commission 2020). The energy in buildings is largely used for heating, ventilation, and air conditioning (HVAC) in order to achieve the necessary air changes and provide a good quality of indoor environment (Zhong et al., 2022). To reduce dependence on fossil fuels, Natural Ventilation (NV) is being widely recognised as an effective means of delivering fresh air and comfort cooling in buildings, but the performance depends greatly on design (Nomura & Hiyama, 2017; Zhong et al., 2022). A well-designed NV system can ensure removal of indoor contaminants, provide thermal comfort and occupant control at a much lower cost compared with a mechanical ventilation system (Belleri et al., 2014; Gupta et al., 2021; Zhong et al., 2022). Designing a NV strategy depends on several factors, such as opening styles, arrangement of the opening, indoor-outdoor condition, wind condition, among others (Wang et al., 2017; Zhong et al., 2022). A building's architectural arrangement is a crucial factor in incorporating a suitable NV strategy in a room. In many cases, such as residential buildings, hostels, and dormitories, openings are possible only on one side of the room, thus falling under the single-sided ventilation category (Gupta et al., 2021). Many studies in the past have focused on the performance of ventilation for single-side natural ventilation for different window configurations, but not so much on the thermal comfort aspects. This study focuses on providing a deeper understanding of efficiently using a CFD simulation tool to replicate wind-driven single-sided NV flow and

choosing different window opening styles based on parameters of ventilation effectiveness and thermal comfort, as per EN-ISO 7730, for draught risk calculations and parameters of thermal discomfort in winter conditions; and the American Society of Heating, Refrigerating and Air-Conditioning Engineers (ASHRAE) Standard 55, for thermal comfort parameters in summer conditions.

In the subsequent sections, the three different window opening types are discussed for wind-driven single-sided natural ventilation flow to evaluate parameters of ventilation effectiveness and thermal comfort for different boundary conditions and geometrical simplifications for high quality CFD simulations.

2. Methodology

A CFD study was conducted for different window configurations to evaluate the flow rates based on different internal-external pressure differences. In this section, the model configuration and geometrical assumptions considered for the CFD analysis are presented, followed by the parameters considered for comparing the performance of different window types.

2.1 Geometric Model and Discretization

In natural ventilation flows, the airflow through an opening is affected by several factors, such as the opening configuration, indoor-outdoor temperature difference, heat sources, room geometry, wind speed, direction, among others.

The geometry of one of the two test chambers of Eurac Research's Façade System Interaction Lab is used for the internal domain (8 m x 4 m x 3 m). To replicate outdoor conditions, an external domain of the size 48 m x 36 m x 12 m is used. It should be noted that the computational domains (Fig. 1) for carrying out the CFD simulations were modeled based on the conclusions of Wang et al. (2018) and Gupta et al. (2021), to accurately replicate the physics of a single-sided wind driven flow, while keeping the computational time within a reasonable range. The resulting blockage ratio of this domain size is 2.8 %, which is below the recommended

limits of 3 % (Blocken, 2015). This ensures a large enough domain for correct development of the airflow (Liu & Niu, 2016).

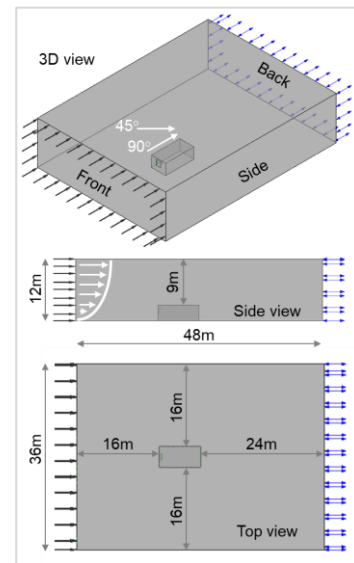


Fig. 1 – CFD model of the domains

For better flexibility, domain discretization is carried out using an unstructured meshing technique, and the mesh is finest at critical points, such as the opening, less coarse for the internal chamber and coarse for the external domain. The meshing technique, as well as the conclusions of the grid independence study inside the chamber, follow the methodology of Gupta et al. (2021). The three different window configurations considered in this study were chosen after a preliminary market analysis (Gupta et al., 2021). Fig. 2 shows the 3 window types and their opening areas. Type_1 (6° open) and Type_2 (20° open) cases have an overall area of 1190 x 1450 mm, and Type_3 (20° open) top-hung fanlight has a top area of 1190 x 450 mm, with a fixed bottom glazed area.

2.2 Basic CFD Principles

The CFD software used a parallel, implicitly coupled multigrid solver. The simulation period was 120 seconds, in transient condition, using steady-state solution for initialisation. An adaptive time-step was used, varying between 10 and 0.5 seconds, as a function of root-mean-square (RMS) courant number of 5, to keep under the residual target within 20 coefficient loops (Babich et al., 2017;

Gupta et al., 2021). A thermal energy transfer is considered, and, since the fluid is air, a Newtonian fluid, Boussinesq approximation was used to consider the buoyancy effects caused due to variations in air density, and was applied by setting up the reference buoyancy temperature equal to the glass temperature (ANSYS Inc., 2013; Babich et al., 2017; Gupta et al., 2021; Wang et al., 2018). The convergence criteria for the RMS residuals was 1e-05 and a conservation target was 0.01 (Babich et al., 2017; Gupta et al., 2021). The Reynolds-averaged Navier–Stokes (RANS) model and SST (Shear Stress Transport) k-omega turbulence model were selected to effectively solve the airflow characteristics (ANSYS Inc. 2013; Gupta et al., 2021; Babich et al., 2017; Zhong et al., 2022). All the simulations were performed with Ansys CFX 2021, and meshing with Ansys ICEM, on a work-station of 16 GB RAM and a 6-core Intel Xenon Gold 6154 CPU.

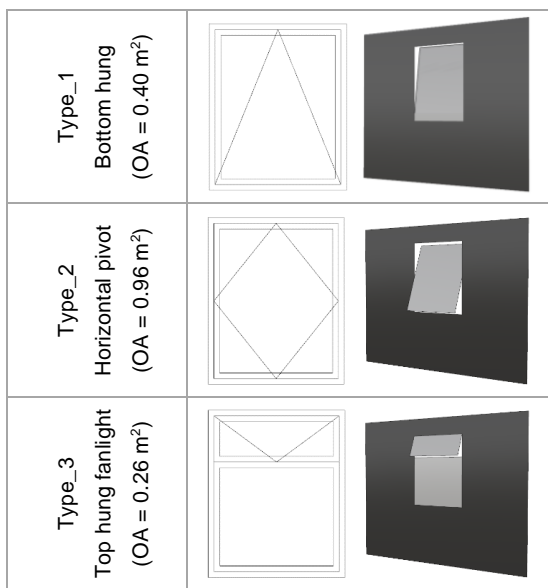


Fig. 2 – Window configurations (OA = opening area)

2.3 Boundary Conditions

Two weather conditions representing typical winter and summer conditions, with internal–external temperature of 20 °C – 10 °C and 30 °C – 25 °C, were considered. Table 1 shows the boundary conditions and temperatures for each domain.

The glass temperature was set to an approximate average of the two domains and is also used as the reference buoyancy temperature as well. The wind force is applied at the front face of the external

domain as an inlet condition, and the wind speed is defined based on the power law, as per Eq. 1:

$$u = u_{ref} \cdot \alpha \cdot (y/y_{ref})^\gamma \quad (1)$$

where u is the wind speed at y height on the surface, and u_{ref} is the reference velocity of 1 m/s, at a reference height of y_{ref} (equal to the Lab height 5 m), as shown in Fig. 1 (side view), and parameters $\alpha=1$, $\gamma=0.143$ refer to a terrain with few trees or small buildings (Wang et al., 2018; Yi et al., 2019).

Table 1 – Boundary conditions and temperatures (air/surface)

Location	Boundary Condition	Temperature	
		Winter	Summer
(a) Chamber Air		20 °C	30 °C
Wall surfaces	No-slip	20 °C	30 °C
Ceiling surface	No-slip	20 °C	30 °C
Floor surface	No-slip	23 °C	30 °C
Window Glass	No-slip	14 °C	28 °C
(b) External Domain Air		10 °C	25 °C
Top surface	Free slip	10 °C	25 °C
Front surface	Inlet	10 °C	25 °C
Ground surface	No-slip	10 °C	25 °C
Side surfaces	Free slip	10 °C	25 °C
Back surface	0Pa opening	10 °C	25 °C
Window Glass	No-slip	14 °C	28 °C

Two wind speeds (1 m/s and 2 m/s), and two wind angles (90°-wind coming perpendicular to the window from the front, and 45°) were chosen for this study, as representative conditions of the region of South Tyrol, Italy. For the wind angle of 45°, the inner domain was rotated for the CFD simulations, as represented in Fig. 1 (3D view), while the external domain remains the same.

2.4 Performance Parameters

The main parameters of ventilation effectiveness and thermal comfort, to compare the performance of different windows, are based on a previous study on buoyancy-driven single sided NV flow (Gupta et al., 2021):

1. Temperature profile – the temperature contour at the vertical plane in the middle of the room.
2. Velocity field – the velocity fields at the same vertical plane in the middle of the room.
3. Incoming airflow rate (Q) – the airflow rate entering the room through the window.

4. Mean Age of Air (MAA) – average time the air entering a building through an opening takes to reach a specific point in the zone (Zhong et al., 2022). It is calculated locally at every point in space, as a scalar quantity in the CFD solver (Gupta et al., 2021).
5. Air changes per hour (ACH) – the total number of times the air inside a space is completely replaced in one hour, as per the Eq. 2:

$$ACH = (Q / V) * 3600 \quad (2)$$
 where Q is the incoming airflow rate (m³/s), and V is the total volume (m³).
6. Effective penetration depth – the longitudinal distance traveled by the air entering from the inlet inside the room. This indicator represents the effective ventilating ability of NV and is an important parameter for single-side ventilated spaces (Zhou et al., 2021). For the context of this study, a maximum length of 8 m is considered.
7. Discharge coefficient (C_d) – this is a function of volume flow rate and pressure difference for a fluid flowing through an opening. It is calculated by rearranging the orifice equation (Yi et al., 2019).

$$C_d = Q / A \cdot \sqrt{\rho/2\Delta p} \quad (3)$$
 where Q is the airflow rate entering the opening (m³/s), A is the opening area (m²), ρ is the air density in the room (kg/m³) and Δp is the difference between the pressure at the opening area and in the room (Pa).
8. Temperature stratification – the difference in temperature along different planes based on EN ISO 7730 and ASHRAE Standard 55, in order to estimate the local thermal discomfort: (a) vertical air temperature difference between the head level (1.8 m from the floor for standing, and 1.1 m from the floor for sitting position) and ankles (0.1 m from floor), and (b) temperature difference at distances 0.5 m, 1 m, 1.5 m and 2 m from the window.
9. Draught risk (DR) – the discomfort caused in winter due to draught is calculated using Eq. 4 (Section 6.2 EN ISO 7730-2005):

$$DR = (34 - t_a) \cdot (v_a - 0.05)^{0.62} (0.37 \cdot v_a \cdot T_u + 3.14) \quad (4)$$
 where t_a is the local air temperature (°C), v_a is the local mean air velocity (m/s), and T_u is the local turbulence intensity (%).

10. Mean air velocity at different heights – the average air velocity at 1.8 m, 1.1 m, and 0.1 m distance above the floor. Based on EN ISO 7730, the effects on the perceived air temperature due to variations in air velocity is evaluated.
11. Mean air velocity near surfaces – this helps to compare the convective heat transfer which is enhanced due to the fluid motion near the surface. Predicting the air velocity near surfaces can be very complicated, but using CFD it can be computed. The air velocity is averaged at a plane 5 cm away from each surface.

3. Results And Discussion

Based on the performance parameters listed in Section 2.4, the results are discussed in this section.

1. Temperature distribution – in Fig. 3 the thermal profiles are presented at the vertical plane in the middle of the room for the wind at a 90° angle. The focus is laid on the inner chamber, without showing the entire external domain. The air enters inside differently according to the different window opening styles and modifies the indoor environment differently. A greater drive of buoyancy is seen at 1 m/s speed, where the colder outdoor wind enters from the lower parts of the window, such as the winter case for Type_1 and Type_2. On the contrary, for 2 m/s wind, the colder wind from outside is dominant and enters through the upper portions. Type_2 shows higher inflow and lower indoor temperatures. In winter conditions, the reduction in the mean indoor temperature for Type_1 at 2 m/s is only 0.6 % higher than the reduction achieved at 1 m/s, whereas for Type_2 this difference is 6.3 %. While in summer, the reduction for Type_1 is only 1.1 %, and for Type_2 is 12.2 %. Type_3 shows a much lower incoming airflow, higher indoor temperature, and a more homogeneous distribution due to low opening area. Up until the part to which the wind penetrates, the profiles are similar to the thermal profiles at the central plane of Wang et al. (2018).

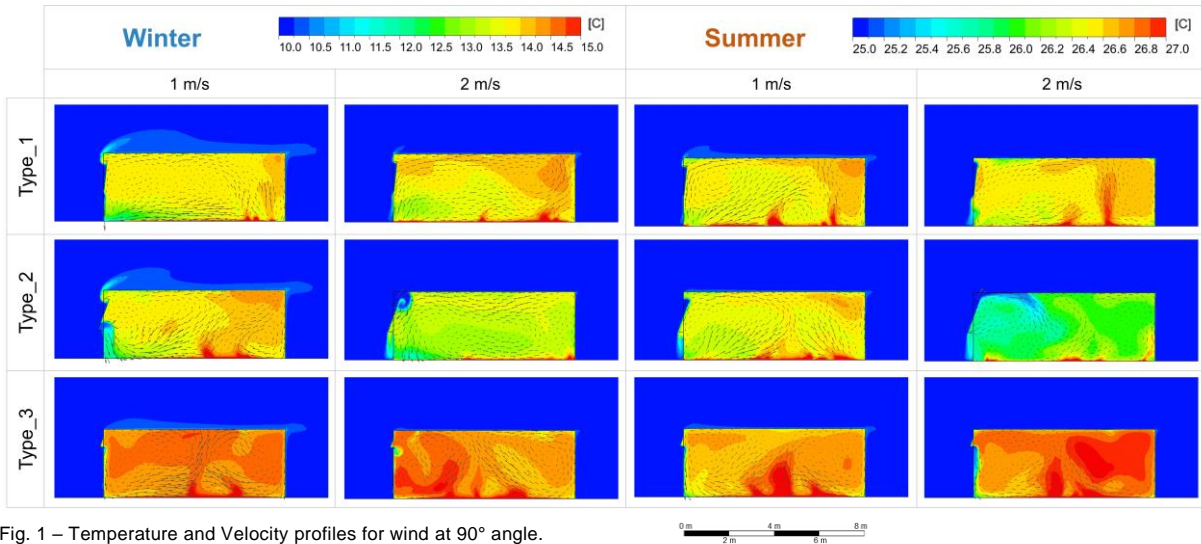


Fig. 1 – Temperature and Velocity profiles for wind at 90° angle.

- Velocity fields – the velocity profile in the inner chamber, for wind at a 90° angle, are shown in Fig. 3. In the winter case, at lower speed, the buoyant forces are dominant, due to high temperature differences. For Type_3, the buoyancy forces are always dominant due to the geometrical configuration of the window, which does not allow the wind to directly enter inside, and the cold air can be seen entering the lower part and immediately falling. Similar fields for these types of windows can be noticed in the results obtained by Wang et al. (2018), but a direct comparison is not possible due to different opening sizes.
- Incoming airflow rate (Q) – as shown in Fig. 4 (a), Q varies largely by the opening types, wind angle and wind speed, and not due to the indoor-outdoor temperature conditions tested. Q for summer and winter conditions do not vary more than 20 %, except for Type_2 for 1 m/s

wind at a 90° angle when Q in summer conditions is 33 % less than in winter conditions. Based on wind speed, Q for 2 m/s wind is always higher than Q for 1 m/s wind, with the minimum difference of 44 % for Type_1 for wind at 45° in winter, up to a maximum of 342 % higher rate for Type_2 for wind at 90° in summer. Based on the angle of wind, Q is always higher for wind at a 45° angle, with a difference of 25 % for Type_1 for 2 m/s wind in summer, up to 210 % for Type_3 for 2 m/s wind in winter and both speeds in summer. This is due to the geometrical advantage of wind coming at an angle and entering indirectly.

- Mean Age of Air (MAA) – as shown in Fig. 4 (b), for the same wind speed and angle, MAA in summer is higher than in winter conditions, because the air changes are slower for lower temperature differences in the summer case, except for Type_2 for 2 m/s wind at a 90° angle where MAA in summer is 17 % lower than in

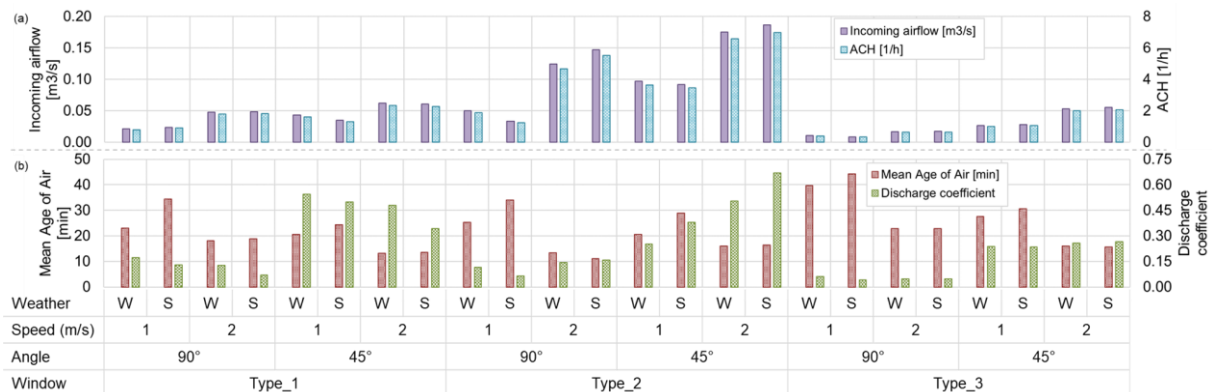


Fig. 2 – Results for (a) incoming airflow and air changes per hour (ACH); (b) mean age of air and discharge coefficient. [W=winter, S=summer]

winter conditions. Based on the wind speed, MAA for 2 m/s is always lower than for 1 m/s wind, from 22 % lower for Type_1 for wind at 90° in winter, as well as for Type_2 for wind at 45° in winter, up to 67 % lower for Type_2 for wind at a 90° angle in summer, due to the corresponding lower Q. For the same wind speed and temperature, MAA for wind at 45° is lower than wind at a 90° angle, except for Type_2 for 2 m/s wind in both weathers.

5. Air changes per hour (ACH) – trends for ACH are observed similar to Q. On comparison with previous studies, ACH for Type_2 shows consistent behavior on increasing wind speed, as well as the range of ACH being consistent for the two wind speeds (Wang et al., 2018).
6. Effective penetration depth – as visible in the velocity profile at the vertical plane in the middle of the room, shown in Fig. 3, it can be observed that the effective penetration depth in all cases varies for each window type, as the influence of the incoming air is different.
7. Discharge coefficient (C_d) – shown in Fig. 4 (b), the C_d of the same type of window varies largely with temperature, wind speed and wind angle, as concluded by previous studies (Heiselberg et al., 2001; Karava et al., 2004; Yi et al., 2019). Based on the wind speed, Type_1 always shows a low C_d for 2 m/s speed, whereas the other Type_2 shows a high C_d at 2 m/s wind. This is due to the geometrical structure of the window opening. Based on the wind angle, C_d is always higher for wind at a 45° angle, with a minimum difference of 118 % for Type_2 for 1 m/s wind in winter, up to 500 % higher for Type_2 for 2 m/s wind in summer. The variation of C_d with wind angle is consistent with the conclusions of Yi et al. (2019), and is due to decreased resistance, as also noticed with the incoming airflow rate.
8. Temperature stratification – the temperature differences at different heights and distances from the window are represented in Fig. 6 (a). More stratification is noticed in winter, due to higher indoor-outdoor temperature difference. The maximum differences at the horizontal and vertical planes are seen for Type_2 in winter for 2 m/s wind at a 90° angle, whereas in the

summer cases, the overall differences are quite low. This shows a good level of air mixing inside the chamber. The temperature differences between head level (1.1 m) and ankles (0.1 m) are in accordance with Category A of ISO 7730, since it is always lower than 2 °C in all cases (Section A.3 EN ISO 7730-2005), and in accordance with ASHRAE 55 (Section 5.3 ASHRAE Standard 55-2017).

9. Draught risk (DR) – Fig. 5 shows the DR and mean indoor temperatures in winter. The maximum DR of 15.8 % is observed for Type_2 at 2 m/s wind at a 45° angle. For the same wind angle, DR is always observed as higher for wind speed 2 m/s, up to 29 % higher for Type_2 for wind at a 90° angle, due to higher mean air velocity indoors. Based on wind angle, DR is always higher for wind at a 45° angle. The thermal environment lies in Category B of the ISO 7730, since DR lies between 10-20 % (Section A.1 EN ISO 7730-2005).
10. Mean air velocity at different heights – as represented in Fig. 6 (b), higher velocity of air is observed at the lowest level of 0.1 m, because of colder air entering and flowing downwards. Based on the ISO 7730, for occupancy similar to office spaces, the maximum mean air velocity lies in Category B for both winter and summer cases (Section A.4 EN ISO 7730-2005).
11. Mean air velocity near surfaces – as per Fig. 6 (b), air velocity is higher near the floor surface and lowest near the ceiling. A maximum of 0.21 m/s is observed near the sidewall for Type_1 for 2 m/s wind at a 45° angle. Due to higher velocity at the floor, a heat source near the floor could be a good option for promoting convective heat transfer, as it is enhanced due to the fluid motion near the surface.

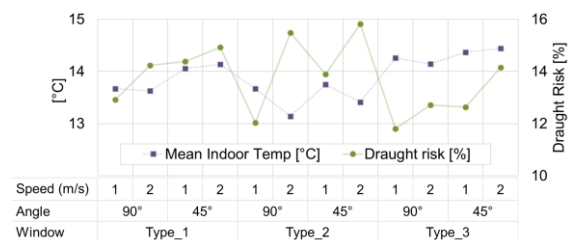


Fig. 5 – Draught risk and mean indoor temperatures in winter for the different window types in different weather conditions

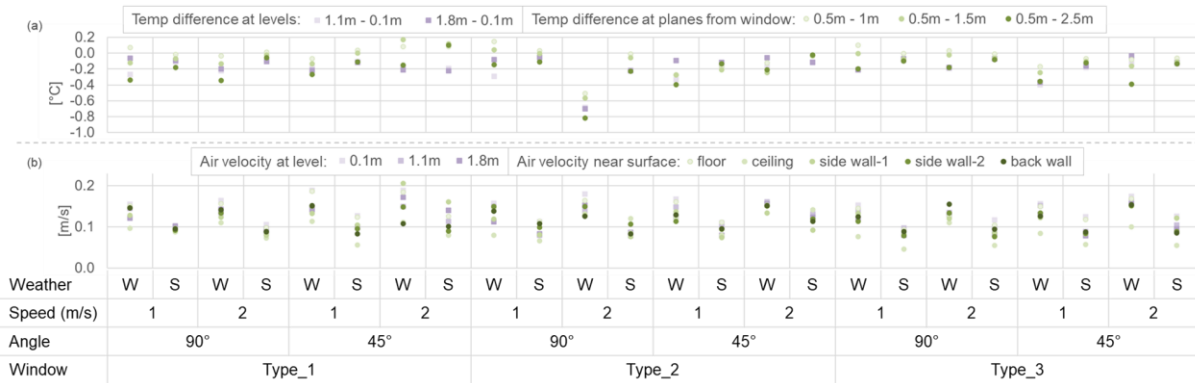


Fig. 6 – Results showing (a) temperature differences at various levels, and (b) air velocity. [W=winter, S=summer]

4. Conclusion

The aim of this study was to investigate the effectiveness of different types of windows for single-sided wind-driven natural ventilation using CFD simulations. A methodology of geometrical modeling of a one-room zone, which is a common condition for student dormitories and many residential apartments with openings only on one side, was studied. The model considered was tested for three different window configurations, two weather conditions, two wind speeds and two different wind angles. The performance of the windows was tested for its ventilation performance, as well as thermal comfort.

It was observed that the ventilation performance is sensitive to the ambient conditions, but for the different opening configurations this sensitivity varies. At low wind speed (1 m/s), the buoyant forces dominate, whereas at higher wind speed (2 m/s), the wind pressure becomes dominant and air enters from the upper portions of the windows. Based on wind speed, for 2 m/s wind, the incoming airflow and air changes per hour are always higher, whereas the mean age of air is always lower when compared with 1 m/s wind. Based on wind angle, for the wind at a 45° angle, the airflow and the air changes per hour are always higher, whereas the mean age of air is generally lower when compared with wind at 90° to the window. The mean age of air in summer is generally higher than in winter, because the air changes are slower for lower temperature differences in the summer case.

The discharge coefficient is dependent on various factors, and the traditional concept of a unique

constant discharge coefficient is not suitable, as the value obtained in the cases modeled was generally below the recommended value of 0.6, which can overestimate the natural ventilation performance. Type_2 (horizontal pivot) shows an increase in discharge coefficient for increasing wind speed, whereas Type_1 (bottom-hung) shows inverse behavior. Based on the wind angle, the discharge coefficient is always higher for wind at a 45° angle. For Type_2 (horizontal pivot) window, higher differences of temperature at different vertical and horizontal places were observed. Based on wind speed, the draught risk is higher for 2 m/s wind, and, based on wind angle, it is higher for wind at a 45° angle. The air velocities are generally high at lower heights, which can promote convective heat transfer.

Therefore, for different window configurations, the aspects of local weather conditions, such as wind speed, angle, indoor-outdoor temperature, should be carefully considered by the designers to better determine ventilation performance and the natural ventilation strategy for each context.

Acknowledgement

The research presented in this paper is supported by funding from the European Regional Development Fund POR FESR 2014-2020 of the Province of Bolzano, under Project number 1116, NEW-AIR: Nuovo approccio per una qualità degli ambienti interni energeticamente efficiente: ricerca e aziende fanno sistema in Alto Adige (English: New approach for an energy efficient IEQ: research and firms systemizing cooperation in South Tyrol).

References

- ANSYS Inc. 2013. "ANSYS CFX Solver Modeling Guide 15.0."
- Babich, F., M. Cook, D. Loveday, R. Rawal, and Y. Shukla. 2017. "Transient Three-Dimensional CFD Modelling of Ceiling Fans." *Building and Environment* 123: 37–49. doi: <https://doi.org/10.1016/J.BUILDENV.2017.06.039>
- Belleri, A., R. Lollini, and S. M. Dutton. 2014. "Natural Ventilation Design: An Analysis of Predicted and Measured Performance." *Building and Environment* 81: 123–38. doi: <https://doi.org/10.1016/J.BUILDENV.2014.06.009>
- Blocken, B. 2015. "Computational Fluid Dynamics for Urban Physics: Importance, Scales, Possibilities, Limitations and Ten Tips and Tricks towards Accurate and Reliable Simulations." *Building and Environment* 91: 219–45. doi: <https://doi.org/10.1016/J.BUILDENV.2015.02.015>
- European Commission. 2020. "Energy Efficiency in Buildings." February 17. https://ec.europa.eu/info/news/focus-energy-efficiency-buildings-2020-lut-17_en
- Gupta, A., A. Belleri, and F. Babich. 2021. "Evaluating the Performance of Different Window Opening Styles for Single-Sided Buoyancy-Driven Natural Ventilation Using CFD Simulations." In *Proceedings of Building Simulation 2021 Conference*. Bruges, Belgium.
- Heiselberg, P., K. Svidt, and P. V. Nielsen. 2001. "Characteristics of Airflow from Open Windows." *Building and Environment* 36(7): 859–69. doi: [https://doi.org/10.1016/S0360-1323\(01\)00012-9](https://doi.org/10.1016/S0360-1323(01)00012-9)
- Karava, P., T. Stathopoulos, and A. K. Athienitis. 2004. "Wind Driven Flow through Openings-A Review of Discharge Coefficients." *International Journal of Ventilation* 3(3). doi: <https://doi.org/10.1080/14733315.2004.11683920>
- Liu, J., and J. Niu. 2016. "CFD Simulation of the Wind Environment around an Isolated High-Rise Building: An Evaluation of SRANS, LES and DES Models." *Building and Environment* 96: 91–106. <https://doi.org/10.1016/J.BUILDENV.2015.11.007>
- Nomura, M., and K. Hiyama. 2017. "A Review: Natural Ventilation Performance of Office Buildings in Japan." *Renewable and Sustainable Energy Reviews* 74: 746–54. doi: <https://doi.org/10.1016/J.RSER.2017.02.083>
- Wang, J., S. Wang, T. Zhang, and F. Battaglia. 2017. "Assessment of Single-Sided Natural Ventilation Driven by Buoyancy Forces through Variable Window Configurations." *Energy and Buildings* 139: 762–79. doi: <https://doi.org/10.1016/J.ENBUILD.2017.01.070>
- Wang, J., T. Zhang, S. Wang, and F. Battaglia. 2018. "Numerical Investigation of Single-Sided Natural Ventilation Driven by Buoyancy and Wind through Variable Window Configurations." *Energy and Buildings* 168: 147–64. doi: <https://doi.org/10.1016/J.ENBUILD.2018.03.015>
- Yi, Q., X. Wang, G. Zhang, H. Li, D. Janke, and T. Amon. 2019. "Assessing Effects of Wind Speed and Wind Direction on Discharge Coefficient of Sidewall Opening in a Dairy Building Model – A Numerical Study." *Computers and Electronics in Agriculture* 162: 235–45. doi: <https://doi.org/10.1016/J.COMPAG.2019.04.016>
- Zhong, H.Y., Y. Sun, J. Shang, F.P. Qian, F.Y. Zhao, H. Kikumoto, C. Jimenez-Bescos, and X. Liu. 2022. "Single-Sided Natural Ventilation in Buildings: A Critical Literature Review." *Building and Environment* 212: 108797. doi: <https://doi.org/10.1016/J.BUILDENV.2022.108797>
- Zhou, J., Y. Hua, Y. Xiao, C. Ye, and W. Yang. 2021. "Analysis of Ventilation Efficiency and Effective Ventilation Flow Rate for Wind-Driven Single-Sided Ventilation Buildings." *Aerosol and Air Quality Research* 21(5): 200383. doi: <https://doi.org/10.4209/AAQR.200383>